Journal of Fluids and Structures (1997) **11,** 535–547

ADAPTIVE MODAL VIBRATION CONTROL OF A FLUID-CONVEYING CANTILEVER PIPE

Y.-K. Tsai and Y.-H. Lin
Department of Mechanical and Marine Engineering, National Taiwan Ocean University Keelung, Taiwan 20224, Republic of China

(Received 1 August 1996 and in revised form 24 March 1997)

A model reference adaptive control approach, designed in the modal space, is applied for flutter control of a cantilever pipe conveying fluid. The control input is provided by a pair of surface-mounted piezoelectric actuators which are driven 180° out of phase to provide an equivalent bending moment acting on the controlled system. Comparison of performance of the model reference adaptive control with that of the optimal independent modal space control reveals that the former is more robust than the latter in terms of flow speed variations, which are unknown in the control system designed; that is, the adaptive approach can tolerate a larger range of flow speed uncertainties without resulting in an unstable control system, so that successful flutter suppression of the fluid-conveying cantilever pipe with high flow speed can be achieved.

1. INTRODUCTION

It has been well known that pipes supported at both ends will buckle when the flow velocity exceeds the critical velocity (Housner 1952; Holmes 1978). For cantilever tubes, flutter instability was observed once the flow velocity exceeds the critical velocity (Gregory & Païdoussis 1966; Païdoussis 1970). In a review article, Païdoussis & Li (1993) demonstrated that analysis of pipes conveying fluid has become a new paradigm in dynamics. Hundreds of papers have been written on the subject and the literature on this topic is constantly expanding.

Despite the intense research efforts towards assessing the dynamical characteristics of pipes conveying fluid, the literature on vibration control of fluid-conveying pipes is quite limited. The study is important to ensure operation accuracy or to prevent catastrophic failure due to excessive vibrations of systems in service, such as oil pipelines, jet-cutting nozzles, and heat-exchanger tubes, etc. Tani & Sudani (1992) reported a sub-optimal control law for vibration suppression of fluid-conveying tubes by using motor-controlled tendons. Sugiyama *et al.* (1992) studied a vibration suppression technique by using an electronic valve to control the internal flowing fluid for a cantilever pipe with sub-critical flow speeds. The valve was used to adjust the speed of the flowing fluid through a feedback on–off control. Yau *et al.* (1992) employed quantitative feedback theory to actively control the excessive vibration of a constrained flexible pipe conveying fluid by using piezoelectric actuators. The control moment was related to the input voltage with an assumed constant. The effects of actuator dynamics were assumed negligible. The analysis was conducted by using a two-degree-of-freedom model. Kangaspuoskari *et al.* (1993) examined the effect of feedback control on critical velocity of cantilevered pipes aspirating fluid. Direct feedback control using displacement, velocity, or acceleration sensors was presented. Since the control design is of the non-collocated type, the system may be unstable

0889–9746/97/050535 + 13 $25.00/fl970092

due to control spillover problems. Recently, Lin & Chu (1996) applied the optimal independent modal space control (IMSC) approach for active flutter suppression of a cantilever pipe conveying fluid. The IMSC approach has been demonstrated to have advantages over the design in physical space, in that it demands far less computer storage, reduces the computational effort significantly, and allows a larger choice of control algorithms, including nonlinear control (Meriovitch *et al.* 1983). The control system designed cannot lose stability due to control spillover from the modes controlled to those uncontrolled by using the IMSC approach. However, it has been observed that while the control is optimal for a particular flow speed, the closed-loop system may become unstable for a small variation of flow speed unknown to the control system.

There has been a considerable amount of interest recently in the application of piezoelectric actuators for sensing and vibration control of flexible structures. Dökmeci (1983a, b, c) surveyed dynamic applications of piezoelectric crystals in view of fundamental, theoretical and experimental studies. Rao & Sunar (1994) reported the recent research trends in using piezoelectricity in sensing and control of flexible structures. This survey covered a broad range of concerns in the fleld, including sensing, actuation, sensitivity and optimization, nonlinear effects, and thermo-piezoelectricity. Crawley (1994) provided an overview and assessment of intelligent structures for aerospace applications. The integration of sensing, actuation, control logic, signal conditioning, and power amplification electronics was discussed.

In the work reported here, a model reference adaptive control approach designed in the modal space is presented. A reference model with asymptotic stability is used to formulate the control design. A feedback gain matrix is adjusted adaptively, which is obtained by solving a set of nonlinear matrix differential equations of size 2×2 for each mode controlled, disregarding how large the model order is. This is in contrast with the design in physical space, which requires solution of full model order nonlinear equations, and may become impractical for higher order systems. Performance of the adaptive control is compared with that of the optimal independent modal space control to examine the robustness of the control system due to unknown variations of the flow speed.

2. FINITE ELEMENT MODEL FORMULATION

Figure 1 depicts the finite element model for the flow-induced vibration problem being considered. Two piezoelectric actuators are bonded on top and bottom of the pipe, respectively. The fluid enters the left end of the tube and exits from the free end. The governing equation of motion is given below, with the detailed formulation for the finite element structural matrices given in the appendix for completeness:

$$\mathbf{M}\ddot{\mathbf{D}}(t) + \mathbf{C}\dot{\mathbf{D}}(t) + \mathbf{K}\mathbf{D}(t) = \mathbf{N}_{x_r}^{\mathrm{T}} M_f(t), \tag{1}$$

where $\mathbf{M}$, $\mathbf{C}$, and $\mathbf{K}$ are the structural mass, damping, and stiffness matrices, respectively, which include the contributions from the support pipe, the piezoelectric actuators, and the moving fluid; $\mathbf{N}_{x_r}^{\mathrm{T}}$ is the transpose of the derivative, with respect to x, of the shape functions evaluated at the right end of the actuators, i.e. x_r in Figure 1; $\mathbf{D}(t)$, $\dot{\mathbf{D}}(t)$ and $\ddot{\mathbf{D}}(t)$ denote displacement, velocity and acceleration vectors, respectively; $M_f(t)$ is the control moment created due to the extension or contraction of the actuators which are driven 180° out of phase. It is known that actuation to the substructure by the piezoelectric actuators when a voltage is applied is equivalent to the moment applied at its ends (Lin & Chu 1994).

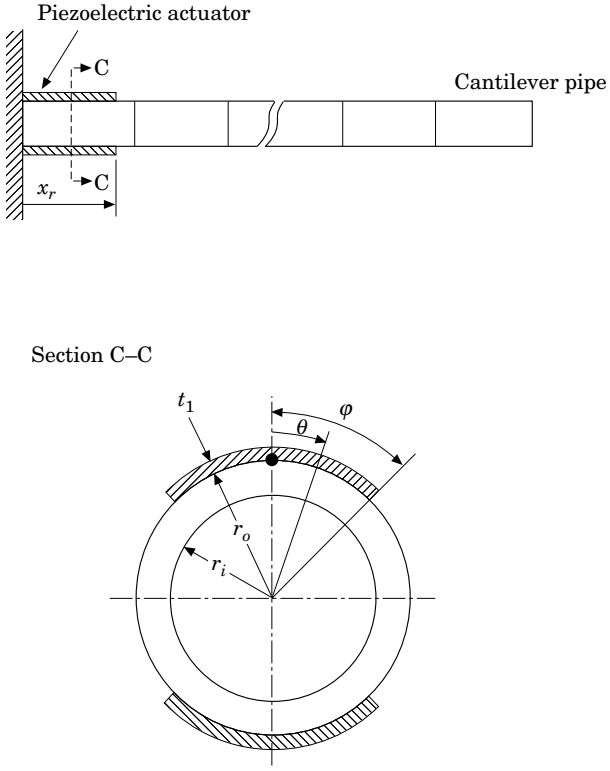

Figure 1. Finite element model of a fluid conveying cantilever pipe with surface mounted piezoelectric actuators.

To facilitate the control formulation, equation (1) is recast to obtain an expression in state space

$$\dot{\mathbf{X}}(t) = \mathbf{A}\mathbf{X}(t) + \mathbf{B}V(t), \tag{2a}$$

where

$$\mathbf{X}(t) = \begin{Bmatrix} \dot{\mathbf{D}}(t) \\ \mathbf{D}(t) \end{Bmatrix}, \tag{2b}$$

$$\mathbf{A} = \begin{bmatrix} -\mathbf{M}^{-1}\mathbf{C} & -\mathbf{M}^{-1}\mathbf{K} \\ \mathbf{I} & \mathbf{0} \end{bmatrix}, \qquad \mathbf{B} = \begin{Bmatrix} \mathbf{M}^{-1}\mathbf{N}_{x_r}^{\mathrm{T}} \\ \mathbf{0} \end{Bmatrix} C_m, \tag{2c,d}$$

in which $V(t)$ is active control input voltage and C_m is a constant to relate the equivalent moment induced from the voltage input. The relationship between the applied voltage and the control moment can be written as

$$M_f(t) = \frac{4\Psi E_A d[(r_o + t_1)^3 - r_o^3] \sin\varphi}{3(1+\Psi)t_1} V(t) = C_m V(t), \tag{3a}$$

where

$$\Psi = \frac{E_P I_P}{E_A I_A}, \tag{3b}$$

in which $E_P I_P$ and $E_A I_A$ are the bending rigidity of the pipe and of the actuator pair, respectively; d is the electric strain constant; and t_1 is the thickness of the piezoelectric actuator. A detailed derivation of equation (3) is given in Lin & Chu (1994).

Equation (2) represents a set of $2n$ first-order differential equations. To decouple equation (2), the concept of biorthogonality between the right and left eigenvectors can be applied (Meirovitch 1980, 1992). By using the following linear transformation, the original state vector $\mathbf{X}(t)$ can be transformed to the modal coordinate $\mathbf{q}(t)$

$$\mathbf{X}(t) = \mathbf{R}\mathbf{q}(t), \tag{4}$$

in which $\mathbf{R}$ is the modal matrix containing the real and imaginary parts of the right eigenvectors (Meirovitch & Ghosh 1987). The following set of decoupled modal equations can be obtained by using the property of biorthogonality:

$$\dot{\mathbf{q}} = \mathbf{\Lambda}\mathbf{q}(t) + \mathbf{Q}_u(t), \tag{5a}$$

where

$$\mathbf{Q}_u(t) = \mathbf{L}^{\mathrm{T}}\mathbf{B}V(t), \tag{5b}$$

in which $\mathbf{L}$ is the modal matrix containing the real and imaginary parts of the left eigenvectors. The modal matrices $\mathbf{L}$ and $\mathbf{R}$ are normalized such that $\mathbf{L}^{\mathrm{T}}\mathbf{R} = \mathbf{I}$. Equation (5) consists of n pairs of decoupled modal equations of the form

$$\dot{\mathbf{q}}_s(t) = \mathbf{\Lambda}_s\mathbf{q}_s(t) + \mathbf{Q}_{u_s}(t), \qquad s = 1, 2, \ldots, n, \tag{6}$$

where

$$\mathbf{q}_s(t) = [\mathbf{q}_{2s-1}(t), \quad \mathbf{q}_{2s}(t)]^{\mathrm{T}},$$

$$\mathbf{\Lambda}_s = \begin{bmatrix} \sigma_s & -\omega_s \\ \omega_s & \sigma_s \end{bmatrix}, \quad \text{and} \quad \mathbf{Q}_{u_s}(t) = [Q_{u_{2s-1}}, \quad Q_{u_{2s}}]^{\mathrm{T}}, \qquad s = 1, 2, \ldots, n. \tag{7}$$

In the following sections both the adaptive and the optimal IMSC methods are discussed. The modal force vector $\mathbf{Q}_{u_s}(t)$ is made to be a function of the sth mode only, and hence complete decoupling of the modal coordinates is achieved. This is the essence of the IMSC method. Note that the modal control design requires estimates of the modal state $\mathbf{q}_s(t)$. For measurements with low noise-to-signal ratios, a Luenberger observer can be used; and for high noise-to-signal ratios, a Kalman–Bucy filter can be applied. The observation spillover can be alleviated by prefiltering the sensor signals to remove the contribution of the uncontrolled modes. Meirovitch & Öz (1980) showed that observation spillover instability can be eliminated by using an appropriate order for the modal state observer.

3. MODAL MODEL REFERENCE ADAPTIVE CONTROL

Adaptive modal vibration control is considered in this work. The modal plant to be controlled adaptively can be described as a linear time-invariant system of order two with unknown parameters and accessible modal states

$$\dot{\mathbf{q}}_s(t) = \mathbf{\Lambda}_s\mathbf{q}_s(t) + \mathbf{B}_s\mathbf{Q}_{u_s}(t), \quad s = 1, 2, \ldots, k, \tag{8}$$

where k is number of modes to be controlled. In general, both $\mathbf{\Lambda}_s$ and $\mathbf{B}_s$ are assumed to be unknown constant matrices. However, $\mathbf{B}_s$ can be regarded as known and is an identity matrix in the present analysis, as can be seen from equations (6) and (8). The reference model used in the adaptive process can be described by the differential equation

$$\dot{\mathbf{q}}_{m_s}(t) = \mathbf{\Lambda}_{m_s}\mathbf{q}_{m_s}(t) + \mathbf{B}_{m_s}\mathbf{r}_s(t), \quad s = 1, 2, \ldots, k, \tag{9}$$

where $\mathbf{\Lambda}_{m_s}$ is a 2×2 asymptotically stable matrix, $\mathbf{B}_{m_s}$ is a 2×2 matrix, and $\mathbf{r}_s(t)$ is a bounded reference input. The matrix $\mathbf{B}_{m_s}$ can be chosen as

$$\mathbf{B}_{m_s} = \mathbf{B}_s\mathbf{\Xi}_s^*, \quad s = 1, 2, \ldots, k, \tag{10}$$

in which Ξ_s^* is a known constant matrix. The modal control input to the plant can then be generated using the following feedback control law (Narendra & Annaswamy 1989):

$$\mathbf{Q}_{u_s}(t) = \boldsymbol{\theta}_s(t)\mathbf{q}_s(t) + \Xi_s^*\mathbf{r}_s(t), \quad s = 1, 2, \ldots, k, \tag{11}$$

where the feedback matrix $\boldsymbol{\theta}_s(t)$ is adjusted adaptively. A constant matrix $\boldsymbol{\theta}_s^*$ is determined using the following relationship:

$$\boldsymbol{\Lambda}_s + \mathbf{B}_s\boldsymbol{\theta}_s^* = \boldsymbol{\Lambda}_{m_s}, \qquad s = 1, 2, \ldots, k. \tag{12}$$

The error differential equations can thus be written as

$$\dot{\mathbf{e}}_s(t) = \boldsymbol{\Lambda}_{m_s}\mathbf{e}_s(t) + \mathbf{B}_s[\boldsymbol{\theta}_s(t) - \boldsymbol{\theta}_s^*]\mathbf{q}_s(t), \qquad s = 1, 2, \ldots, k, \tag{13a}$$

where

$$\mathbf{e}_s(t) = \mathbf{q}_s(t) - \mathbf{q}_{m_s}(t), \qquad s = 1, 2, \ldots, k. \tag{13b}$$

A Lyapunov function for the present system can be expressed as

$$V_s(\mathbf{e}_s, \boldsymbol{\Phi}_s) = \mathbf{e}_s^{\mathrm{T}}\mathbf{P}_s\mathbf{e}_s + \mathrm{Tr}\,[\boldsymbol{\Phi}_s^{\mathrm{T}}\boldsymbol{\Gamma}_s^{-1}\boldsymbol{\Phi}_s], \tag{14a}$$

in which $\mathbf{P}_s$ and the adaptive gain $\boldsymbol{\Gamma}_s$ are symmetric positive-definite matrices, and

$$\boldsymbol{\Phi}_s(t) = \boldsymbol{\theta}_s(t) - \boldsymbol{\theta}_s^*. \tag{14b}$$

The adaptive gain matrix can be expressed as

$$\dot{\boldsymbol{\theta}}_s(t) = \dot{\boldsymbol{\Phi}}_s(t) = -\boldsymbol{\Gamma}_s\mathbf{B}_s^{\mathrm{T}}\mathbf{P}_s\mathbf{e}_s\mathbf{q}_s^{\mathrm{T}}. \tag{15}$$

Differentiating equation (14) leads to

$$\dot{V}_s(\mathbf{e}_s, \boldsymbol{\Phi}_s) = -\mathbf{e}_s^{\mathrm{T}}\mathbf{Q}_{0_s}\mathbf{e}_s \leq 0, \tag{16a}$$

which indicates that energy is dissipating, and

$$-\mathbf{Q}_{0_s} = \boldsymbol{\Lambda}_{m_s}^{\mathrm{T}}\mathbf{P}_s + \mathbf{P}_s\boldsymbol{\Lambda}_{m_s}. \tag{16b}$$

Note that in the present analysis the initial conditions of the reference model are set to zero and the tracking force vector $\mathbf{r}_s(t)$ is null; that is, the control is of the regular type. The states of the reference model will then be identically zero. The control law as shown in equation (15) assures that

$$\lim_{t\to\infty}[\mathbf{q}_s(t) - \mathbf{q}_{m_s}(t)] = 0. \tag{17}$$

Therefore, the states of the plant will be adaptively regulated to zero as time unfolds.

4. OPTIMAL INDEPENDENT MODAL SPACE CONTROL

The modal cost function for each mode controlled is defined as

$$J_s = \int_0^\infty \{\mathbf{q}_s^{\mathrm{T}}(t)\mathbf{q}_s(t) + \mathbf{Q}_{u_s}^{\mathrm{T}}(t)\mathbf{E}_s\mathbf{Q}_{u_s}(t)\}\,\mathrm{d}t, \qquad s = 1, 2, \ldots, k. \tag{18}$$

It has been shown by Lin & Chu (1995) that if the weighting matrix $\mathbf{E}_s$ is not properly chosen, as in Meirovitch & Baruh (1981) and Meirovitch & Ghosh (1987), the closed-loop system may lead to instability, depending on how the complex eigenvectors are normalized. The use of a diagonal weighting matrix with identical elements

alleviates such problems and the associated Riccati matrix for optimal control action becomes

$$\mathbf{S}_s = \begin{bmatrix} \bar{S}_s & 0 \\ 0 & \bar{S}_s \end{bmatrix}, \qquad s = 1, 2, \ldots, n, \tag{19}$$

where the closed form solution can be shown to be

$$\bar{S}_s = \sigma_s E_{s11} + \sqrt{E_{s11}(E_{s11}\sigma_s^2 + 1)}\,, \qquad s = 1, 2, \ldots, k, \tag{20}$$

in which E_{s11} is the diagonal element of the weighting matrix $\mathbf{E}_s$. In contrast with the adaptive control input shown in equation (11), the optimal independent modal space control leads to a control input law (Lin & Chu 1995):

$$\begin{bmatrix} Q_{u_{2s-1}}(t) \\ Q_{u_{2s}}(t) \end{bmatrix} = \begin{bmatrix} \bar{S}_s/E_{11} & 0 \\ 0 & \bar{S}_s/E_{s11} \end{bmatrix} \begin{bmatrix} q_{2s-1}(t) \\ q_{2s}(t) \end{bmatrix}, \qquad s = 1, 2, \ldots, n. \tag{21}$$

5. SIMULATION RESULTS

The numerical data for this simulation study, as used in the work by Lin & Chu (1996) are: (a) for the pipe: Young's modulus 68·9 GPa, length 10 m, mass per unit length 0·342 kg/m, pipe diameter 0·0254 m, and wall thickness 0·00165 m; (b) for the actuator: Young's modulus 45 GPa, length 1·25 m, thickness 0·0005 m, angle $\varphi = 85°$, piezoelectric constant -260×10^{-12} m/volt, and mass density 7600 kg/m^3. The mass per unit length of the fluid is 0·0858 kg/m. The initial conditions of the adaptive feedback gain matrix $\boldsymbol{\theta}_s(t)$ are taken to be null. A total of eight elements are used to describe the model dynamics. Performance of the adaptive control system for a cantilever pipe conveying fluid with flow speed $1{\cdot}1v_{cr}$ is illustrated in Figure 2, where v_{cr} is the critical flow speed to cause flutter instability in the second mode. Since the second mode dominates the dynamic response, it is targeted as the mode to be controlled. The pipe was displaced 0·01 m initially at the free end. The effect of the adaptive gain matrix $\boldsymbol{\Gamma}_s$ on system response is clearly demonstrated in Figure 2. For the case of gain $\boldsymbol{\Gamma}_s = 50\,000\mathbf{I}$, vibration of the pipe is virtually eliminated after $t/\tau = 12$, where τ is the traveling time of a fluid particle from one end of the pipe to the other, whereas the

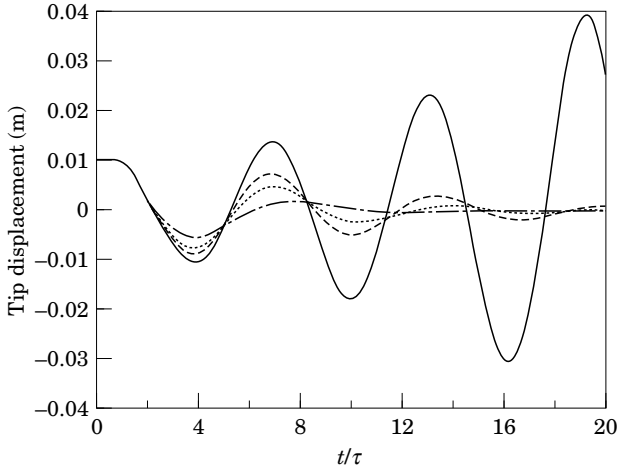

Figure 2. Calculated vertical tip responses for various adaptive gains with flow speed $v = 1{\cdot}1v_{cr}$: (——), uncontrolled; (– – –), $\boldsymbol{\Gamma}_s = 10\,000\mathbf{I}$; (· · ·), $\boldsymbol{\Gamma}_s = 20\,000\mathbf{I}$; (— · —), $\boldsymbol{\Gamma}_s = 50\,000\mathbf{I}$.

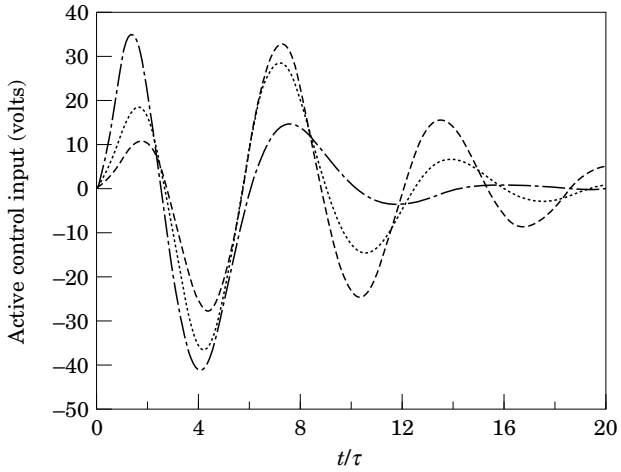

Figure 3. Calculated active control input voltages for various adaptive gains with flow speed $v = 1{\cdot}1v_{cr}$: (– – –), $\mathbf{\Gamma}_s \times 10\,000\mathbf{I}$; (· · ·), $\mathbf{\Gamma}_s = 20\,000\mathbf{I}$; (— · —), $\mathbf{\Gamma}_s = 50\,000\mathbf{I}$.

uncontrolled system exhibits flutter instability. The associated active control input voltages are shown in Figure 3, which indicates that only a small amount of input voltage is required to suppress excessive vibration of the pipe for the present analysis case. If the flow speed, initial disturbances, or the adaptive gain matrix $\mathbf{\Gamma}_s$ are larger, the control input voltage will become higher accordingly.

Note that the control input is designed to control the second mode. However, control spillover from the mode controlled to the modes uncontrolled exists when discrete actuators are used. The spillover effect is accounted for by solving equation (5b) to obtain $V(t)$ after the modal inputs, $\mathbf{Q}_{u_s}(t)$, is synthesized from the control design, and the physical control moment can then be obtained from equation (3a), which is used in equation (1) to compute the system responses. An alternative way to account for the spillover effect is to compute the modal forces for those modes uncontrolled and solve equation (5a) for the modal responses. The physical response can then be obtained from equation (4). The two approaches yield identical results. For the present analysis, the control spillover effect was found to be insignificant.

Figure 4 shows the performance of the optimal IMSC system for various flow speeds. The control system is designed for the critical flow speed. Therefore, the control system reacts without knowing the speed variations. For flow speeds less than the critical one, vibration of the pipe is suppressed rapidly, since the uncontrolled pipe vibrates less violently than that for which the control system was originally designed. For flow speeds above $1{\cdot}2v_{cr}$, the system vibrates so violently and its dynamic behavior has deviated from the one designed so much that the control system is unable to regulate the pipe vibration to the equilibrium state. The associated active control input voltages are shown in Figure 5. Performance of the adaptive independent modal space control for various flow speeds is shown in Figure 6. Since the control law of the adaptive scheme is different from that of the previous optimal IMSC approach, the adaptive gain was adjusted so that the controlled system responses are as close as possible between the two approaches for the critical flow speed. As can be seen in Figure 6, even at the high flow speed of $v = 1{\cdot}5v_{cr}$, the adaptive control system is still capable of regulating excessive vibration of the fluid-conveying pipe back to the equilibrium state. The corresponding active control input voltages are illustrated in Figure 7. Note that for

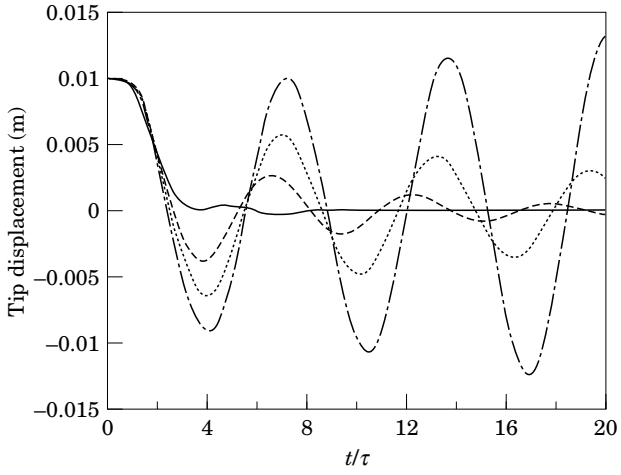

Figure 4. Calculated vertical tip responses with the use of the optimal IMSC approach; system designed for the critical flow speed and $\mathbf{E}_s = 0{\cdot}5\mathbf{I}$; (——), $v = 0{\cdot}8v_{cr}$; (– – –), $v = v_{cr}$; (· · ·), $v = 1{\cdot}1v_{cr}$; (— · —), $v = 1{\cdot}2v_{cr}$.

the case of $v = 1{\cdot}5v_{cr}$ the peak control voltage is close to the coercive field of the actuators, and hence further increase of flow speed, which demands higher control input, is not recommended for the present control configuration.

It is apparent that the adaptive IMSC scheme has the ability to tolerate larger variations of flow speeds, not known to the control system, than that of the optimal IMSC approach, at the expense of the need to solve the matrix equation (15) in real time. However, the matrix equation is only of size 2×2 for each mode controlled in the present modal design approach, disregarding how large the model order is. Therefore, real-time computing is feasible to carry out the control design. Note that if the control system knows the flow speed exactly and is specifically designed for that speed, the optimal IMSC approach performs the best, as its name implies.

Figure 8 shows the effect of the initial conditions of the adaptive feedback gain

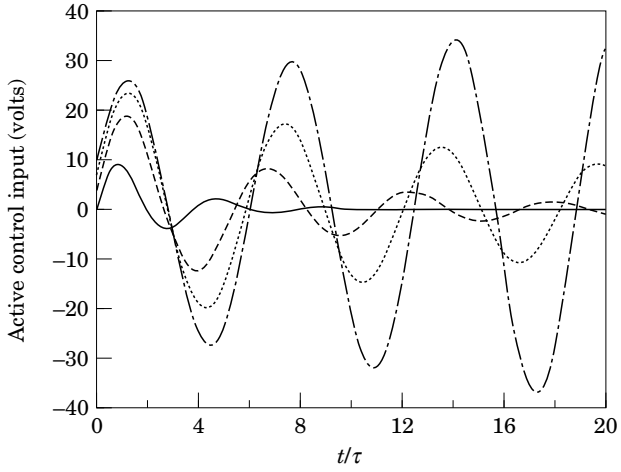

Figure 5. Calculated active control input voltages with the use of the optimal IMSC approach; system designed for the critical flow speed and $\mathbf{E}_s = 0{\cdot}5\mathbf{I}$. (——), $v = 0{\cdot}8v_{cr}$; (– – –), $v = v_{cr}$; (· · ·), $v = 1{\cdot}1v_{cr}$; (— · —), $v = 1{\cdot}2v_{cr}$.

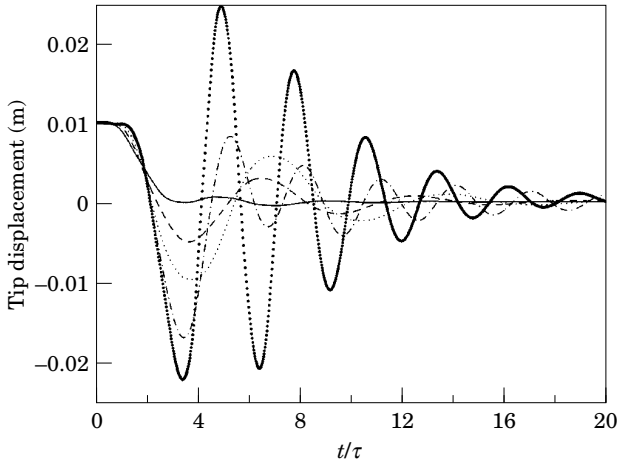

Figure 6. Calculated vertical tip responses with the use of the adaptive IMSC approach; system designed for the critical flow speed and $\mathbf{\Gamma}_s = 20\,000\mathbf{I}$. (——), $v = 0{\cdot}8v_{cr}$; (– – –), $v = v_{cr}$; (· · ·), $v = 1{\cdot}2v_{cr}$; (— · —), $v = 1{\cdot}4v_{cr}$; (• • •), $v = 1{\cdot}5v_{cr}$.

matrix $\boldsymbol{\theta}_s(t)$ on the dynamic response of the pipe system. The associated control input voltages are illustrated in Figure 9. As can be seen, the system response becomes more violent in the start-up when $\boldsymbol{\theta}_s(0)$ is higher. In this analysis, the limit of the control input is set to ± 500 volts so as not to exceed the field capacities of the actuators and the power amplification circuits. The operation range can be increased if better actuators and higher capacity of amplifiers are used. For the case of $\boldsymbol{\theta}_s(0) = 20\mathbf{I}$, the control input saturates and the dynamic response at the pipe tip can be found to be more than four times the initial displacement disturbance magnitude at start-up. The adaptive controller is still capable of regulating the system back to the equilibrium position under such a situation. However, as noted by an anonymous reviewer of this work, further increase of $\boldsymbol{\theta}_s(0)$ will make the saturation problem more severe, which

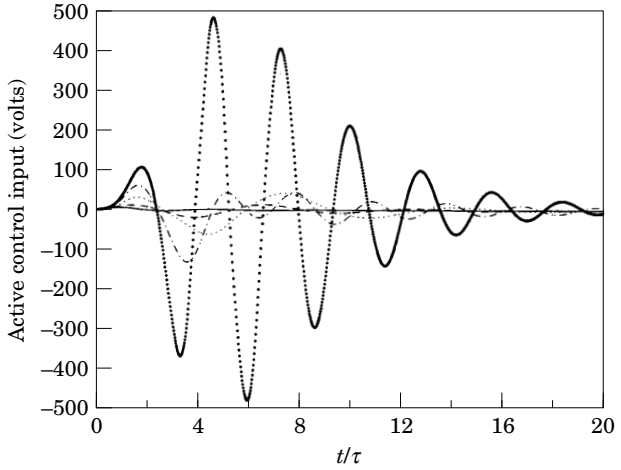

Figure 7. Calculated active control input voltages with the use of the adaptive IMSC approach; system designed for the critical flow speed and $\mathbf{\Gamma}_s = 20\,000\mathbf{I}$. (——), $v = 0{\cdot}8v_{cr}$; (– – –), $v = v_{cr}$; (· · ·), $v = 1{\cdot}2v_{cr}$; (— · —), $v = 1{\cdot}4v_{cr}$; (• • •), $v = 1{\cdot}5v_{cr}$.

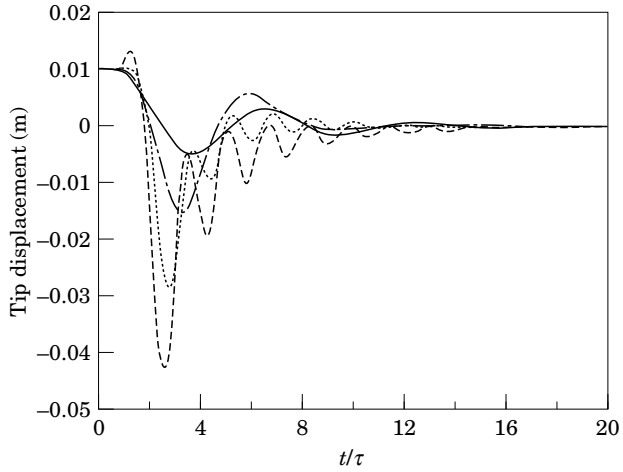

Figure 8. Calculated vertical tip responses at the critical flow speed with the use of the adaptive IMSC approach, $\mathbf{\Gamma}_s = 20\,000\mathbf{I}$. (——), $\boldsymbol{\theta}_s(0) = \mathbf{0}$; (— · —), $\boldsymbol{\theta}_s(0) = 5\mathbf{I}$; (· · ·), $\boldsymbol{\theta}_s(0) = 10\mathbf{I}$; (– – –), $\boldsymbol{\theta}_s(0) = 20\mathbf{I}$.

ultimately leads to system instability because the control input is no longer supplied as designed. Therefore a proper choice of $\boldsymbol{\theta}_s(0)$ is crucial to ensure stability and performance of the control system.

6. CONCLUSIONS

Active flutter suppression of a cantilever pipe conveying fluid with high flow speeds by using the model reference adaptive control approach in modal space has been presented in this work. Only a set of matrix nonlinear differential equations of size 2×2 needs to be solved for each mode controlled by using the adaptive modal control scheme, whereas the ordinary adaptive control law in physical space requires the solution of a set of nonlinear equations with full model order, which may be prohibitive for higher order systems. It has been shown that the adaptive modal control is more

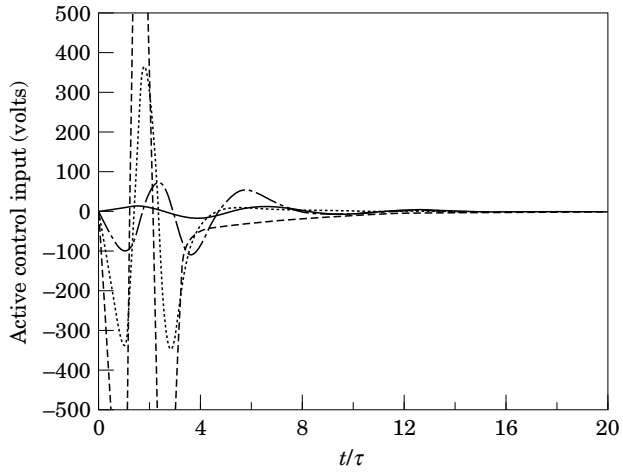

Figure 9. Calculated active control input voltages at the critical flow speed with the use of the adaptive IMSC approach, $\mathbf{\Gamma}_s = 20\,000\mathbf{I}$. (——), $\boldsymbol{\theta}_s(0) = \mathbf{0}$; (— · —), $\boldsymbol{\theta}_s(0) = 5\mathbf{I}$; (· · ·), $\boldsymbol{\theta}_s(0) = 10\mathbf{I}$; (– – –), $\boldsymbol{\theta}_s(0) = 20\mathbf{I}$.

robust than the optimal independent modal space control for flow speed variations unknown to the control system. For the case analysed in this study it is demonstrated that the present control configuration is capable of suppressing flutter of the cantilever pipe conveying fluid, even with 50% variation of higher flow speed from that for which it was designed.

It should be stressed that this paper mainly aimed to show that the proposed adaptive control scheme can work, rather than that it *will* work (and adapt) under all conceivable situations. Adaptive schemes must be used with care, and their stability, the effect of disturbances and noise, parameter uncertainty and so on, need to be tested–something that was not done here, but could be the subject of further studies into the usefulness of this control scheme under more realistic conditions. Other future research areas include optimization of the actuator location, incorporation of a more accurate model for the fluid–structure interactions, and control approaches for pipes with rapid time-varying flow speeds.

ACKNOWLEDGMENT

The authors are grateful to the National Science Council (NSC), Taiwan, R.O.C., for the financial support under the contract NSC 85-2212-E-019-002.

References

Chu, C.-L. & Lin, Y.-H. 1995 Finite element analysis of fluid-conveying Timoshenko pipes. *Shock and Vibration* **2,** 247–255.

Crawley, E. F. 1994 Intelligent structures for aerospace: a technology overview and assessment. *AIAA Journal* **32,** 1689–1699.

Cook, R. D. 1976 *Concepts and Applications of Finite Element Analyis,* Second edition. New York: John Wiley & Sons.

Dökmeci, M. C. 1983a Dynamic applications of piezoelectric crystals. Part I: Fundamentals. *Shock and Vibration Digest,* **15,** 9–20.

Dökmeci, M. C. 1983b Dynamic applications of piezoelectric crystals. Part II: Theoretical studies. *Shock and Vibration Digest,* **15,** 15–26.

Dökmeci, M. C. 1983c Dynamic applications of piezoelectric crystals. Part III: Experimental studies. *Shock and Vibration Digest,* **15,** 11–22.

Gregory, R. W. & Païdoussis, M. P. 1966 Unstable oscillations of tubular cantilevers conveying fluid. Parts 1 and 2. *Proceedings of the Royal Society of London,* Series A **293,** 512–542.

Holmes, P. J. 1978 Pipes supported at both ends cannot flutter. *Journal of Applied Mechanics* **45,** 619–622.

Housner, G. W. 1952 Bending vibrations of a pipe line containing flowing fluid. *Journal of Applied Mechanics* **19,** 205–208.

Kangaspuoskari, M., Laukkanen, J. & Pramila, A. 1993 The effect of feedback control on critical velocity of cantilevered pipes aspirating fluid. *Journal of Fluids and Structures* **7,** 707–715.

Lin, Y.-H. & Chu, C.-L. 1994 Comments on active modal control of vortex-induced vibrations of a flexible cylinder. *Journal of Sound of Vibration* **175,** 135–137.

Lin, Y.-H. & Chu, C.-L. 1995 A new design for independent modal space control of general dynamic systems. *Journal of Sound and Vibration* **180,** 351–361.

Lin, Y.-H. & Chu, C.-L. 1996 Active flutter control of a cantilever tube conveying fluid using piezoelectric actuators. *Journal of Sound and Vibration* **196,** 97–105.

Lin, Y.-H. & Treathewey, M. W. 1990 Finite element analysis of elastic beams subjected to moving dynamic loads. *Journal of Sound and Vibration* **136,** 323–342.

McIver, D. B. 1973 Hamilton's principle for systems of changing mass. *Journal of Engineeering Mathematics* **7,** 249–261.

Meirovitch, L. 1980 *Computational Methods in Structural dynamics.* The Netherlands: Sijthoff & Noordhoff.

MEIROVITCH, L. 1992 *Dynamics and Control of Structures.* New York: John Wiley & Sons.
MEIROVITCH, L. & BARUH, H. 1981 Optimal control of damped flexible gyroscopic systems. *Journal of Guidance and Control* **4,** 157–163.
MEIROVITCH, L., BARUH, H. & ÖZ, H. 1983 A comparison of control techniques for large flexible systems. *Journal of Guidance and Control* **6,** 302–310.
MEIROVITCH, L. & GHOSH, D. 1987 Control of flutter in bridges. *ASCE Journal of Engineering Mechanics* **113,** 720–736.
MEIROVITCH, L. & ÖZ, H. 1980 Modal-space control of distributed gyroscopic systems. *Journal of Guidance and Control* **3,** 140–150.
NARENDRA, K. S. & ANNASWAMY, A. M. 1989 *Stable Adaptive Systems.* Englewood Cliffs: Prentice-Hall.
PAÏDOUSSIS, M. P. 1970 Dynamics of tubular cantilevers conveying fluid. *I. Mech. E. Journal of Mechanical Engineering Science* **12,** 85–103.
PAÏDOUSSIS, M. P. & LI, G. X. 1993 Pipes conveying fluid: A model dynamical problem. *Journal of Fluids and Structures* **7,** 137–204.
RAO, S. S. & SUNAR, M. 1994 Piezoelectricity and its use in disturbance sensing and control of flexible structures: a survey. *Applied Mechanics Reviews* **47,** 113–123.
SUGIYAMA, Y., KATAYAMA, T., KANKI, E., NISHINO, K. & ÅKESSON, B. 1992 Stabilization of cantilevered flexible structures by means of an intenal flowing fluid controlled by an electronic valve. *ASME/JSME/CSME/IMechE/IAHR International Symposium on Flow-Induced Vibration & Noise,* Vol. 8 (eds M. P. Païdoussis & N. S. Namachchivaya), AMD-Vol. 152, pp. 79–86. ASME: New York. An updated version was published in *Journal of Fluids and Structures* **10,** 653–661 (1996).
TANI, J. & SUDANI, Y. 1992 Active flutter suppression of a tube conveying fluid. *The First European Conference on Smart Structures and Materials,* pp. 333–336.
YAU, C.-H., BAJAJ, A. K. & NWOKAH, O. D. I. 1992 Active control of chaotic vibration in a constrained flexible pipe conveying fluid. *ASME/JSME/CSME/IMechE/IAHR International Symposium on Flow-Induced Vibration & Noise,* Vol. 8 (eds M. P. Païdoussis & N. S. Namachchivaya), AMD-Vol. 152, pp. 93–108. ASME: New York. An updated version was published in *Journal of Fluids and Structures* **9,** 99–122 (1995).

APPENDIX

The finite element method is applied in this research to study the feasibility of active vibration control of a flexible pipe conveying fluid. The formulation of the finite element model for both the support pipe and the moving fluid is briefly described here. The transverse displacement of the pipe is described by the element nodal degrees of freedom with a set of interpolating functions (Cook 1976),

$$w = \lfloor N \rfloor \{d\}_e, \tag{A1}$$

where $\lfloor N \rfloor$ denotes 1×4 row vectors representing shape functions, $\{d\}_e$ the element nodal degrees of freedom vector including transverse displacements and rotations, and

$$\lfloor N \rfloor = \lfloor N_1 \quad N_2 \quad N_3 \quad N_4 \rfloor, \tag{A2}$$

in which

$$\begin{aligned} N_1 &= 1 - 3\left(\frac{x}{l}\right)^2 + 2\left(\frac{x}{l}\right)^3, \\ N_2 &= x\left(\frac{x}{l} - 1\right)^2, \\ N_3 &= 3\left(\frac{x}{l}\right)^2 - 2\left(\frac{x}{l}\right)^3, \\ N_4 &= x\left[\left(\frac{x}{l}\right)^2 - \frac{x}{l}\right], \end{aligned} \tag{A3}$$

where 'l' denotes the pipe element length, and 'x' the coordinate along the longitudinal direction of the pipe element. The pipe element mass and stiffness matrices can be obtained using the standard finite element procedure (Cook 1976):

$$[m]_e = \int_0^l \lfloor N \rfloor^T \rho A \lfloor N \rfloor \, dx, \tag{A4}$$

$$[k]_e = \int_0^l EI \lfloor N \rfloor_{xx}^T \lfloor N \rfloor_{xx} \, dx, \tag{A5}$$

where ρ and A denote the mass per unit volume and the cross-section of the pipe element, respectively; EI is the bending rigidity. The element mass and stiffness matrices of the piezoelectric actuators can be obtained similarly.

The development of a finite element model for fluid moving on a flexible pipe is described below. By denoting the coordinate of the fluid as $w_0\ (x, t)$ and that of the support pipe as $w(x, t)$ and knowing that they are the same at the contact position, the time derivatives of w_0 can be described as (Lin and Trethewey 1990)

$$\begin{aligned} \ddot{w}_0(x, t) &= w_{xx}\dot{x}^2 + 2w_{xt}\dot{x} + w_x\ddot{x} + w_{tt} \\ &= w_{xx}v^2 + 2w_{xt}v + w_x\dot{v} + w_{tt}, \end{aligned} \tag{A6}$$

in which a subscript denotes partial differentiation; v is the fluid flow velocity and its overdot denotes the acceleration. From equation (A1), the following relationship can be established

$$\begin{aligned} w_{xx} &= \lfloor N \rfloor_{xx}\{d\}, \qquad & w_{xt} &= \lfloor N \rfloor_x\{\dot{d}\}, \\ w_x &= \lfloor N \rfloor_x\{d\}, \qquad & w_{tt} &= \lfloor N \rfloor\{\ddot{d}\}. \end{aligned} \tag{A7}$$

Equations (A6) and (A7) can be combined and integrated over the element span, by considering the virtual work done by the fluid inertia forces, to obtain the element mass, damping, and stiffness matrices for the fluid moving at a constant velocity as below (Chu & Lin 1995):

$$\begin{aligned} [m_f]_e &= \mu_f \int_0^l \lfloor N \rfloor^T \lfloor N \rfloor \, dx, \\ [c_f]_e &= 2\mu_f v \int_0^l \lfloor N \rfloor^T \lfloor N \rfloor_x \, dx - \mu_f v \lfloor N \rfloor^T \lfloor N \rfloor \Big|_{x=0}^{x=l}, \\ [k_f]_e &= \mu f v^2 \int_0^l \lfloor N \rfloor^T \lfloor N \rfloor_{xx} \, dx - \mu_f v^2 \lfloor N \rfloor^T \lfloor N \rfloor_x \Big|_{x=0}^{x=l}, \end{aligned} \tag{A8}$$

where μ_f is the mass per unit length of the fluid. The last terms on the right-hand side of the damping and stiffness matrix expressions, which are not attributed to those described in equation (A6), represent the inflow terms at $x = 0$, and the outflow terms at $x = l$, as the fluid enters the pipe element from one end and exits from the other to account for the fluid boundary conditions (McIver 1973). The above finite element matrices for the pipe, the actuators, and the moving fluid can be assembled to form the structural matrices for analysis. Note that at the free end of the pipe, the outflow terms as described above need to be added to the structural matrices for correct formulation.